Supporting Information for

Light-Triggered Evolution of Molecular Cluster toward Sub-nanoscale Heterojunction with High Interface Density

Chaozhuang Xue,[a] Jiaxu Zhang,[a] Xiang Wang,[a] Meng Gu,[b] Yuanmin Zhu,[b,c] Dong-Sheng Li,[d] Jun Guo,[e] Yang Liu,[f] and Tao Wu*[a]

[a] *College of Chemistry, Chemical Engineering and Materials Science, Soochow University, Suzhou, Jiangsu 215123, China*

[b] *Department of Materials Science and Engineering, Southern University of Science and Technology, Shenzhen, 518055, China*

[c] *Academy for Advanced Interdisciplinary Studies, Southern University of Science and Technology, Shenzhen, 518055, China*

[d] *College of Materials and Chemical Engineering, Hubei Provincial Collaborative Innovation Center for New Energy Microgrid, Key Laboratory of Inorganic Nonmetallic Crystalline and Energy Conversion Materials, China Three Gorges University, Yichang, 443002, China*

[e] *Testing & Analysis Center, Soochow University, Suzhou, Jiangsu, 215123, China*

[f] *Key Lab of Bioorganic Phosphorus Chemistry and Chemical Biology, Department of Chemistry, Tsinghua University, Beijing 100084, China*

Chemicals and Materials. Zinc acetate dihydrate (Zn, 99%, powder), sulfur (S, 99.9%, powder), pyridine (Py, > 99%, liquid), 3,5-dimethylpyridine (3,5-DMPy, > 99%, liquid), N, N-dimethylformamide (DMF > 99%, liquid), ethanol (> 99%, liquid) and deionized water were used as received without further purification.

Synthesis of ZSP-1. Zinc acetate dihydrate (60 mg), sulfur (30 mg) and pyridine (1.5 mL) and DMF (0.5 mL) were added to a 5 mL glass tube. The vessel was sealed and shaked up at room temperature, then heated at 120 °C for 2 days. The tube was subsequently allowed to cool to room temperature, and then colorless regular rhombic prism crystals were obtained with the yield of 35 mg (76 % based on Zn source).

Synthesis of L-ZnOS. 30 mg of **ZSP-1** powder was added into 100 mL deionized water and ultrasonically treated for 10 min at room temperature. Then, the mixture was transfered to photocatalytic reactor. While the reactor was vacuumized to 1.0 kPa at low temperature (5 °C), the system was under the illumination of Xe lamp for five hours without any filter applied. The final suspension was centrifuged with 10000 rpm and the sediment was washed by ethanol for three times for the following characterizations.

Synthesis of H-ZnS and H-ZnOS. H-ZnS and **H-ZnOS** were synthesized by heating as-synthesized **ZSP-1** in the tube furnace for two hours under air condition at 300 °C and 600 °C, respectively. The tube furnace was subsequently allowed to cool to room temperature.

Structure characterization. Single-crystal X-ray diffraction measurements were performed on Bruker Photon II CPAD diffractometer with nitrogen-flow temperature controlled using graphite-monchromated Mo-*Kα* (λ =0.71073 Å) radiation at 120 K. The structure was solved by direct method using SHELXS-2014 and the refinement against all reflections of the compound was performed using SHELXL-2014. SADABS-2016/2 (Bruker AXS area detector) was used for absorption correction. The values of R(int) before and after the absorption correction were 0.1292 and 0.0499 respectively. The Ratio of minimum to maximum transmission is 0.8962. The lambda/2 correction factor is 0.0015. Solvent masking was performed on mask program in olex2 to squeeze the solvent (water). Powder X-ray diffraction (PXRD) data were collected on a desktop diffractometer (D2 PHASER, Bruker, Germany) using Cu-Kα (λ=1.54084 Å) radiation operated at 30 kV and 10 mA.

Elemental analysis. Energy dispersive spectroscopy (EDS) analysis was performed on scanning electron microscope (SEM) equipped with energy dispersive spectroscopy (EDS) detector. An accelerating voltage of 25 kV and 40 s accumulation time were applied. Elemental analysis of C, H and N was performed on VARIDEL III elemental analyzer.

Thermogravimetric measurement. A Shimadzu TGA-50 thermal analyzer was used to measure TG curve by heating the sample from room temperature to 600 °C with heating rate of 5 °C /min under N_2

flow.

Optical measurements. Room-temperature solid-state UV-Vis diffusion reflectance spectra of crystal samples were collected on a SHIMADZU UV-3600 UV-Vis-NIR spectrophotometer by using $BaSO_4$ powder as the reflectance reference. The absorption spectra were calculated from reflectance spectra by using the Kubelka-Munk function: $F(R)=\alpha/S=(1-R)^2/2R$, where R, α, and S are the reflection, the absorption and the scattering coefficient, respectively. To determine band edge of the direct-gap semiconductor, the relation between the absorption coefficients (α) and the incident photon energy (h) is exhibited as $\alpha h\upsilon = A\,(h\upsilon - Eg)^{1/2}$, where A is a constant that relates to the effective masses associated with the valence and conduction bands, and Eg is the optical transition gap of the solid material. The band gap of the obtained samples can be determined from the Tauc plot with $[F(R)*h\upsilon]^2$ vs. $h\upsilon$ by extrapolating the linear region to the abscissa.

Photoelectrochemical experiment. To prepare the electrode, 2 mg of crystalline samples were first ground into fine powder by using a marble and pestle, and then added into 200 μL of 0.5 % nafion (5% in water and isopropanol). After ultrasonic treatment for 10 minutes, the obtained suspensions were dropped onto the surface of ITO substrate, and then dried at room temperature. The photocurrent experiments were performed on a CHI760E electrochemistry workstation in standard three-electrode configuration, with the sample coated ITO glass (the effective area is around 1 cm^2) as the working electrode, a Pt electrode as the auxiliary electrode, and a saturated calomel electrode (SCE) as the reference electrode. The light source is a 150 W high pressure xenon lamp, located 20 cm away from the surface of the ITO electrode. Sodium sulfate aqueous solution (0.5 M, 100 mL) was used as the supporting electrolyte.

Photoluminescence (PL) characterization. Photoluminescence (PL) spectra were recorded on a HORIBA scientific Fluorolog-3 spectrofluorometer with corresponding accessories.

Photocatalytic experiments. The photocatalytic H_2 generation reaction was analyzed in a closed gas circulation system. 20 mg of the sample was dispersed in a 100 mL aqueous solution containing Na_2S (0.01 M, 2.4 g) and Na_2SO_3 (0.01 M, 2.4 g) as the sacrificial reagent. After vacuumed to 1.0 kPa at low temperature (5 °C), the suspension was irradiated under a 300 W xenon lamp. During the photocatalytic reaction, the reaction solution was kept with a continuous magnetic stirring and at 5 °C by a flow of cooling water. The evolved gases were analyzed by gas chromatography equipped with a thermal conductive detector and N_2 as carrier gas.

TEM measurements. TEM and HRTEM were conducted on a HITACHI HT7700 transmission electron microscope (TEM) at an acceleration voltage of 120 kV and FEI Tecnai F20 TEM at an acceleration voltage of 200 kV. The samples were prepared by dropping dispersion of particle/piperidine/ethanol onto carbon-coated copper TEM grids and dried under ambient condition.

HAADF-STEM imaging and electron energy loss spectroscopy (EELS) were conducted using an aberration-corrected Transmission Electron Microscopy (Titan Themis Z60-300) operated at an accelerating voltage of 300 kV, equipped with Gatan 965 spectrometer.

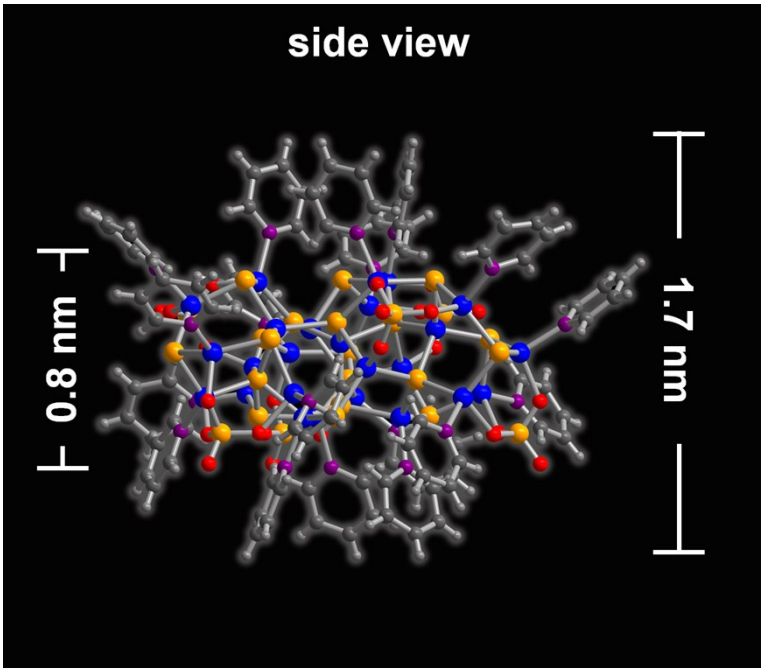

Fig. S1 Ball-and-stick model of side-viewed Zn-S-O cluster in **ZSP-1**.

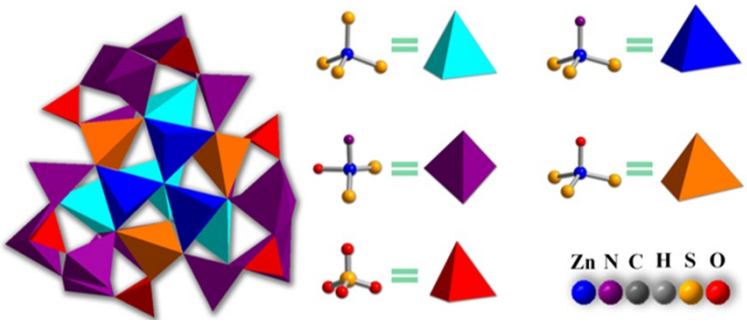

Fig. S2 Four coplanar ZnS_4 tetrahedra are fused together via vertex-sharing sulfur to form a pinwheel pattern capped by three ZnS_3N and three ZnS_3O tetrahedra, which is further covered by fifteen ZnS_2NO tetrahedra to give a flabellum-like structure.

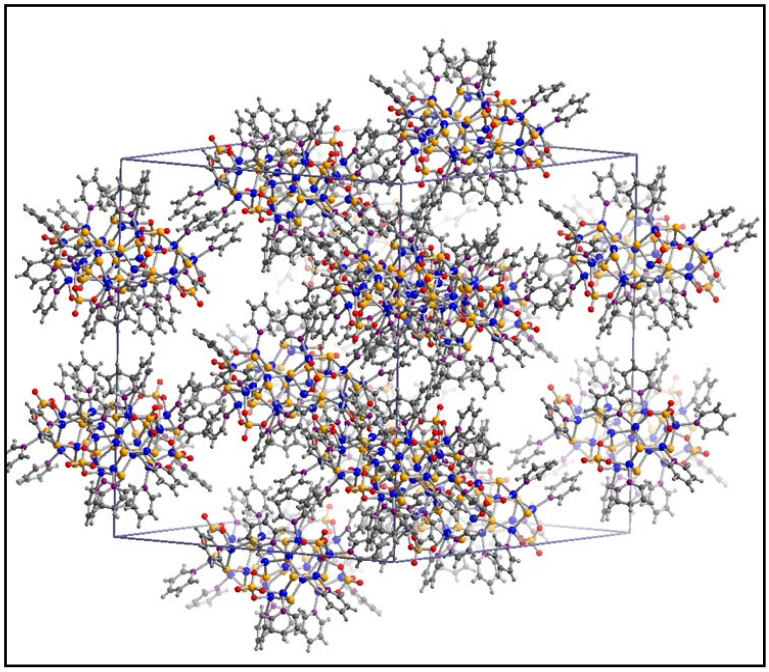

Fig. S3 3D packing diagram of Zn-S-O clusters in **ZSP-1**. The driving forces for the cluster packing should be van der Waals forces and π-π force.

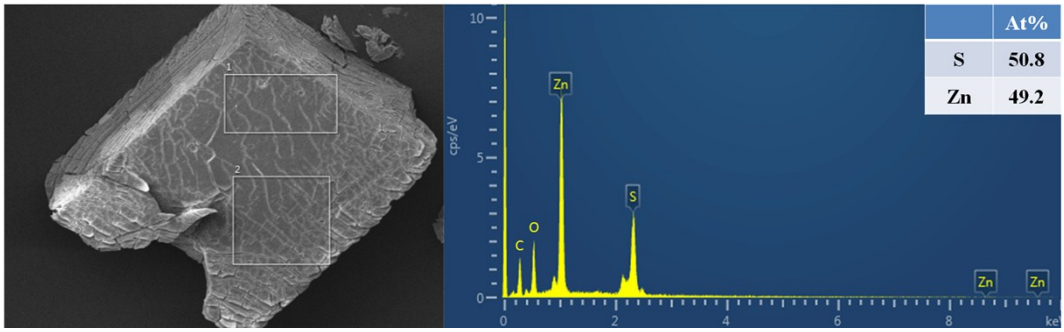

Fig. S4 SEM image and EDS result of **ZSP-1**.

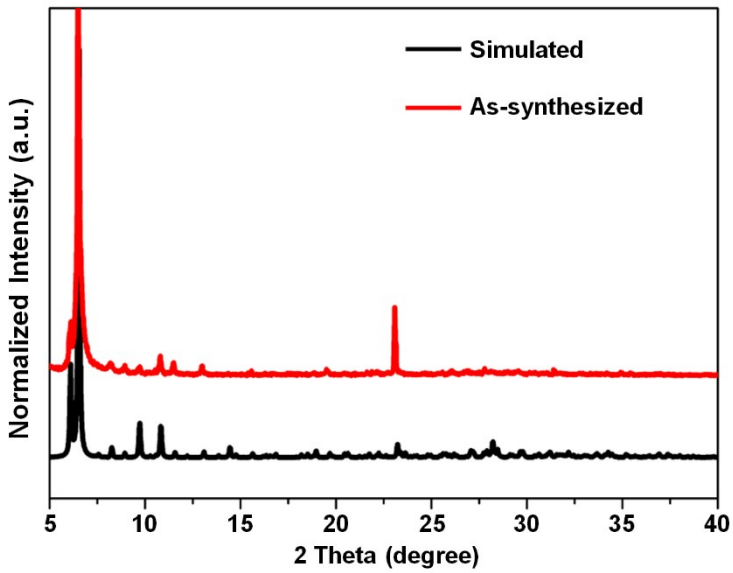

Fig. S5 PXRD patterns for as-synthesized **ZSP-1** and the simulated one.

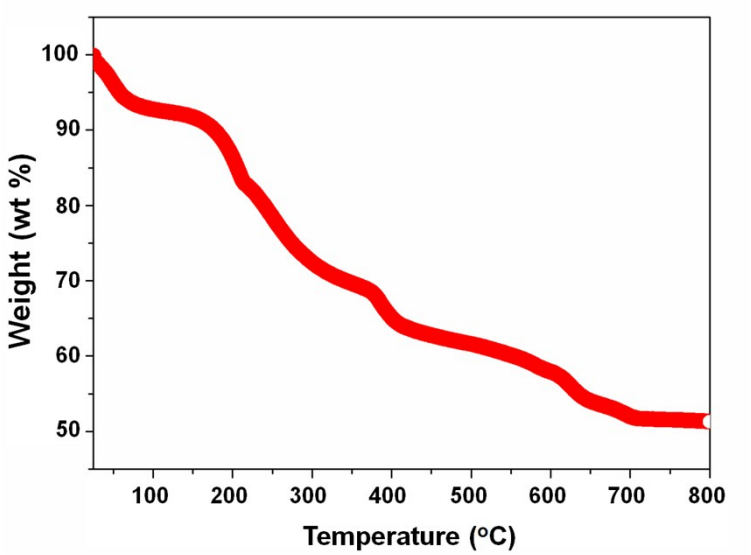

Fig. S6 TGA curve of **ZSP-1** under N_2 atmosphere.

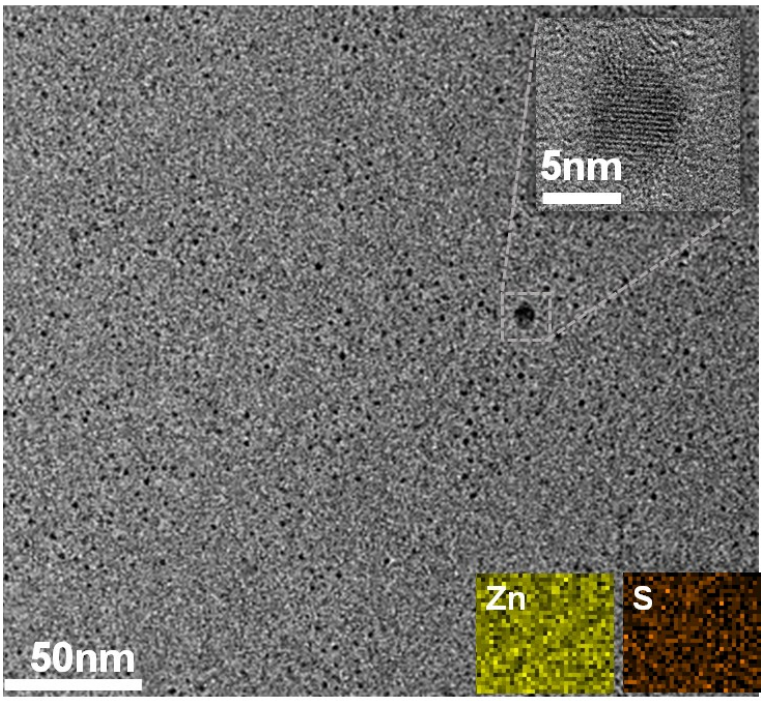

Fig. S7 TEM image of the dispersed **ZSP-1**. The inset is HRTEM image and EDS mapping.

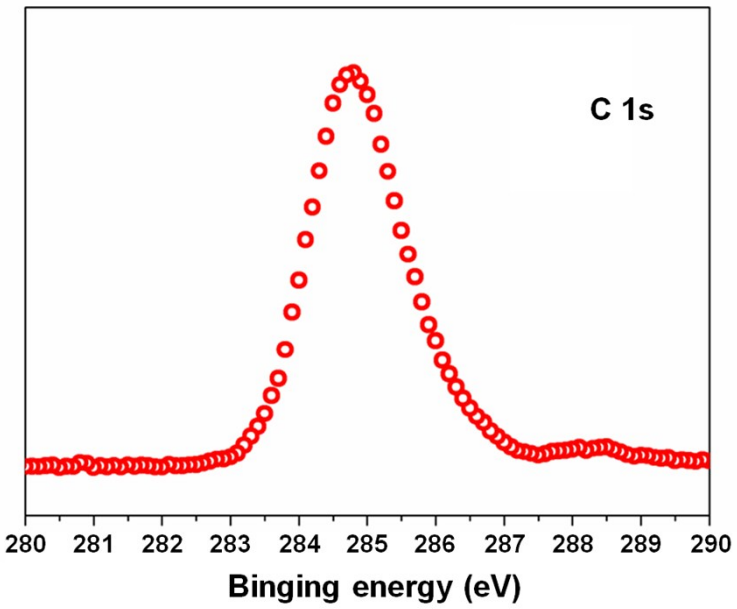

Fig. S8 HRXPS spectra corresponding to C 1s for pristine **ZSP-1**.

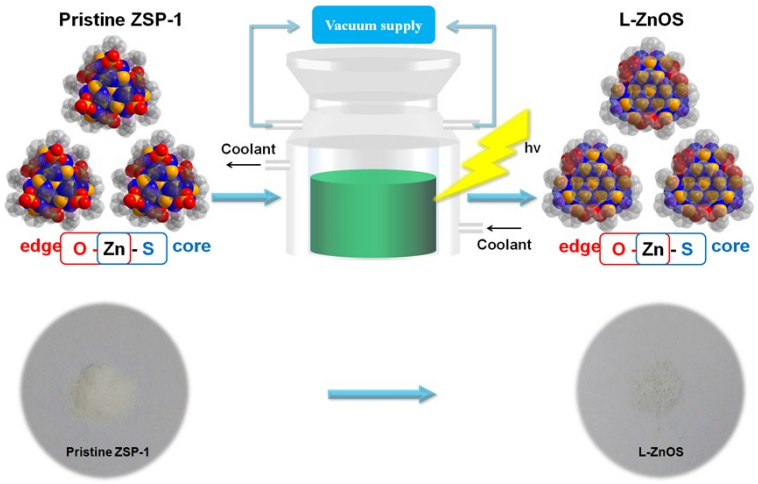

Fig. S9 The schematic diagram of light treatment on the dispersed **ZSP-1** sample.

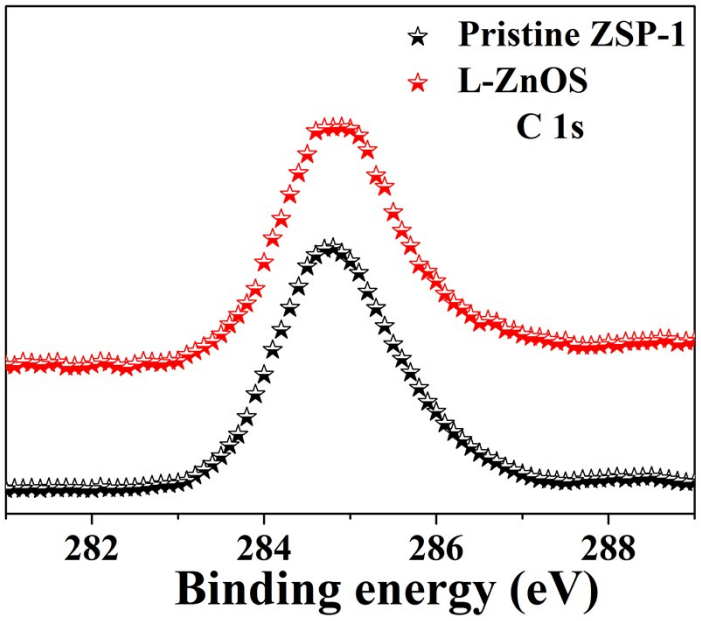

Fig. S10 Comparison of HRXPS spectra corresponding to C1s for **ZSP-1** and **L-ZnOS**.

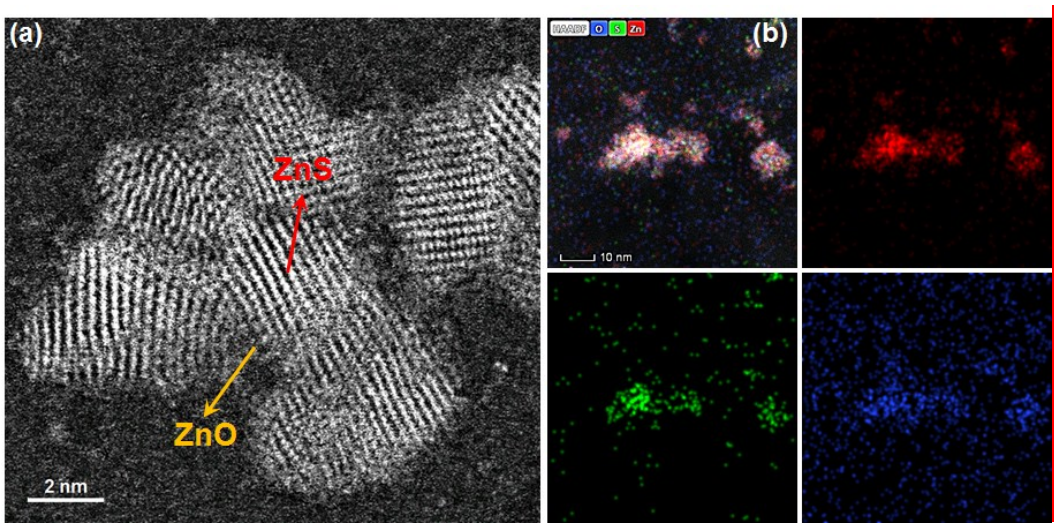

Fig. S11 (a) High-angle annular dark-field scanning TEM (HAADF-STEM) image. ZnS phase with clear lattice surrounded by amorphous ZnO phase. (b) STEM-EELS mapping of L-ZnOS particle: Zn K edge mapping in red, S L2,3 edge mapping in green, O K edge mapping in blue and the integrated mapping of Zn, S and O are shown.

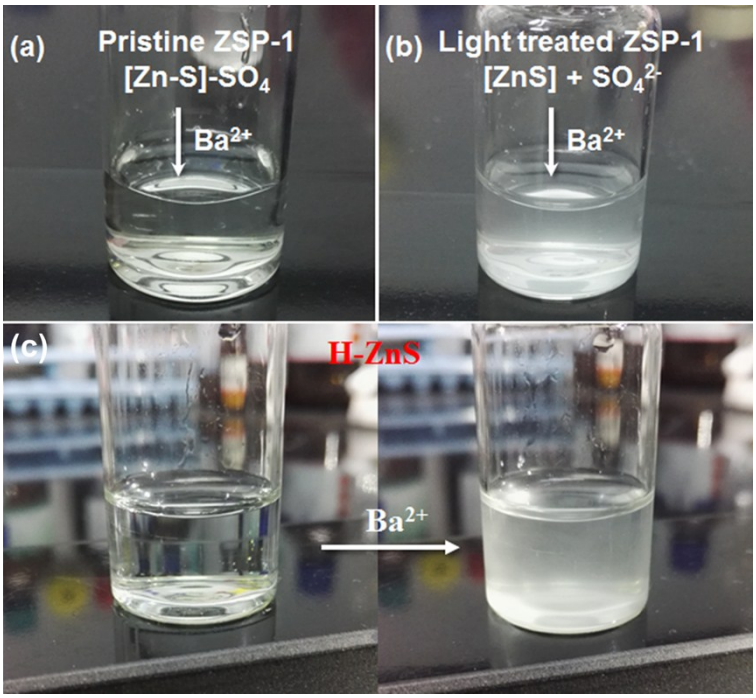

Fig. S12 The qualitative SO_4^{2-} detection on the aqueous suspensions of pristine **ZSP-1** (a), light-treated **ZSP-1** (b) and heat-treated sample (c) by using Ba^{2+} as detecting ions.

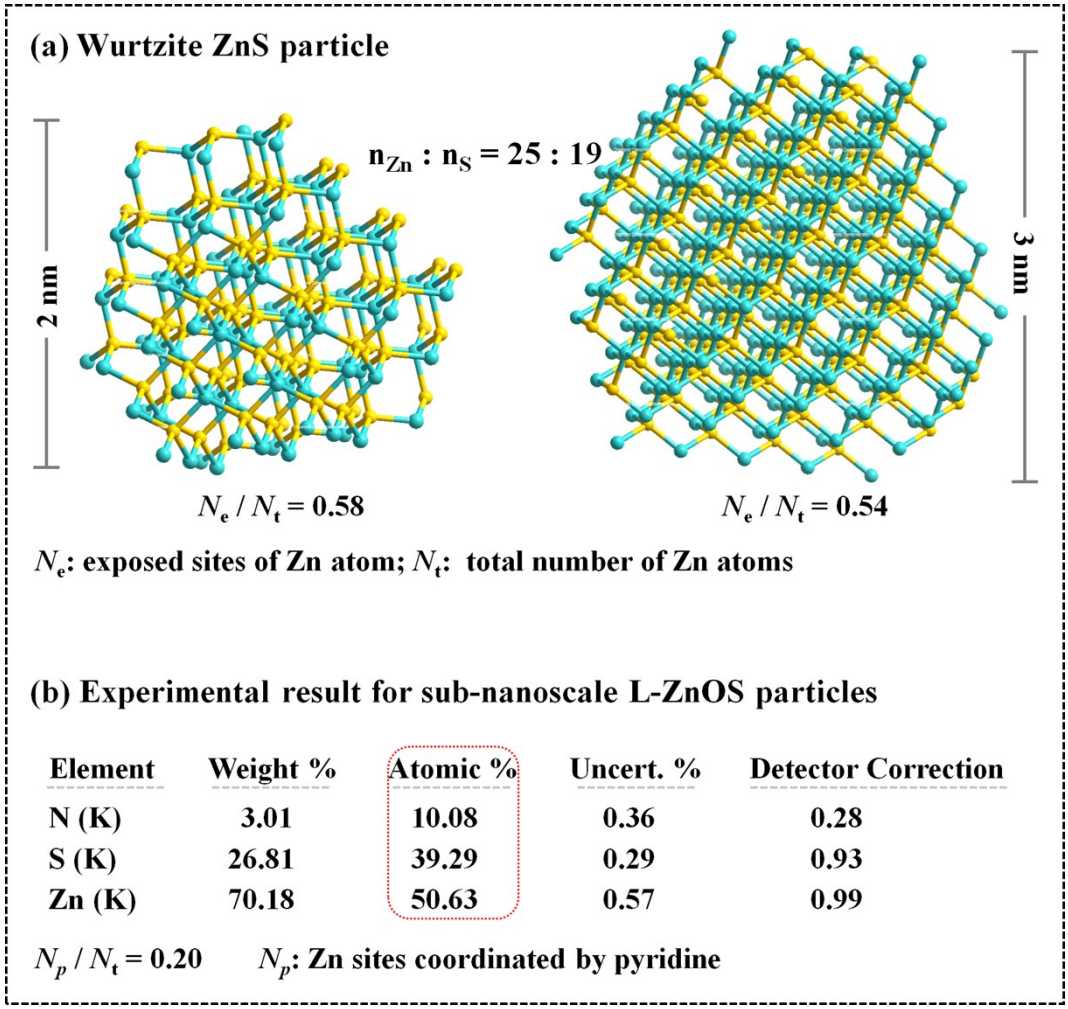

Fig. S13 (a) Geometric models of wurtzite ZnS nanoparticle with Zn sites exposed. (b) Elements analysis for sub-nanoscale **L-ZnOS** nanoparticles.

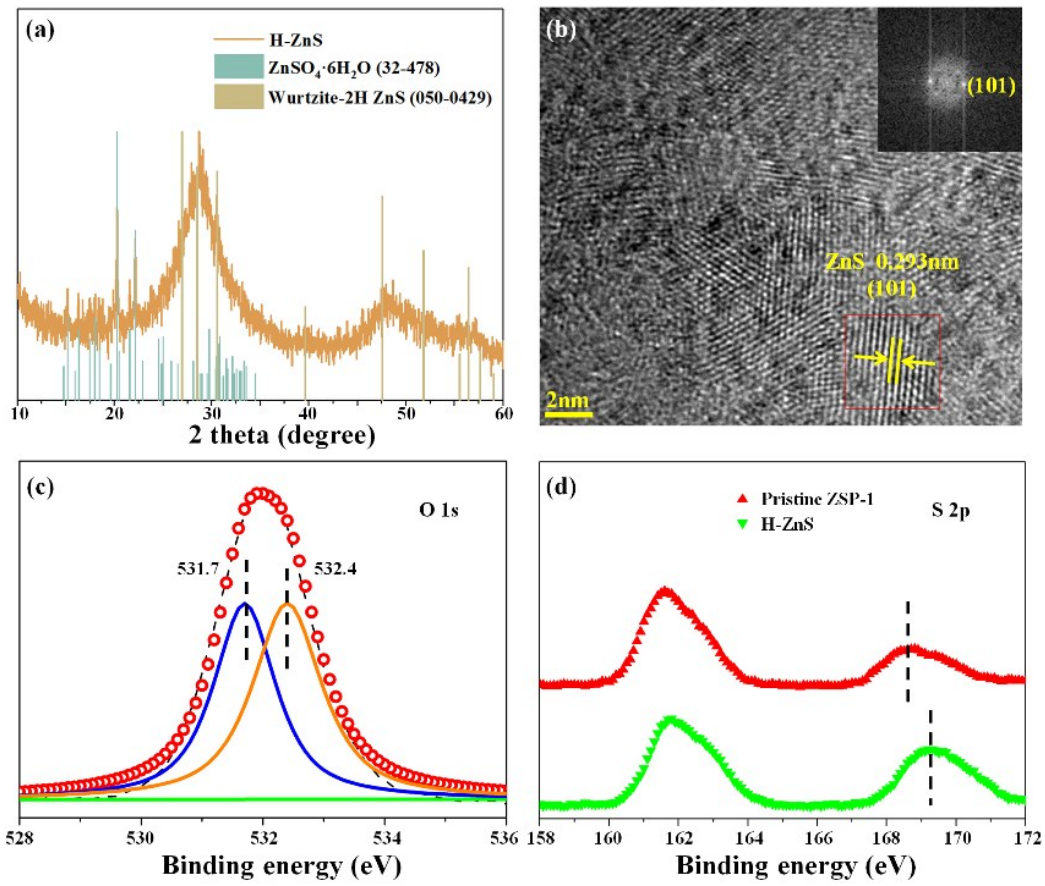

Fig. S14 (a) PXRD pattern of **H-ZnS** match well with JCPDS of $ZnSO_4 \cdot 6H_2O$ and wurtzite-2H ZnS. (b) HRTEM image of **H-ZnS**. The lattice spacing of 0.293 nm is indexed to the characteristic (101) plane of wurtzite-2H ZnS, and the inset is the image of the corresponding selected area electron diffraction. (c) HRXPS spectra corresponding to O1s of **H-ZnS**. Zn-O related sub-peak in pristine **ZSP-1** disappeared, indicating the dissociation of SO_4^{2-} groups from host cluster. (d) HRXPS spectra corresponding to S 2p of **H-ZnS**. Compared to that in **ZSP-1**, SO_4^{2-}-related peak at bonding energy of 169.2 eV is obviously blue-shifted, which is caused by dissociation of SO_4^{2-} groups from host cluster.

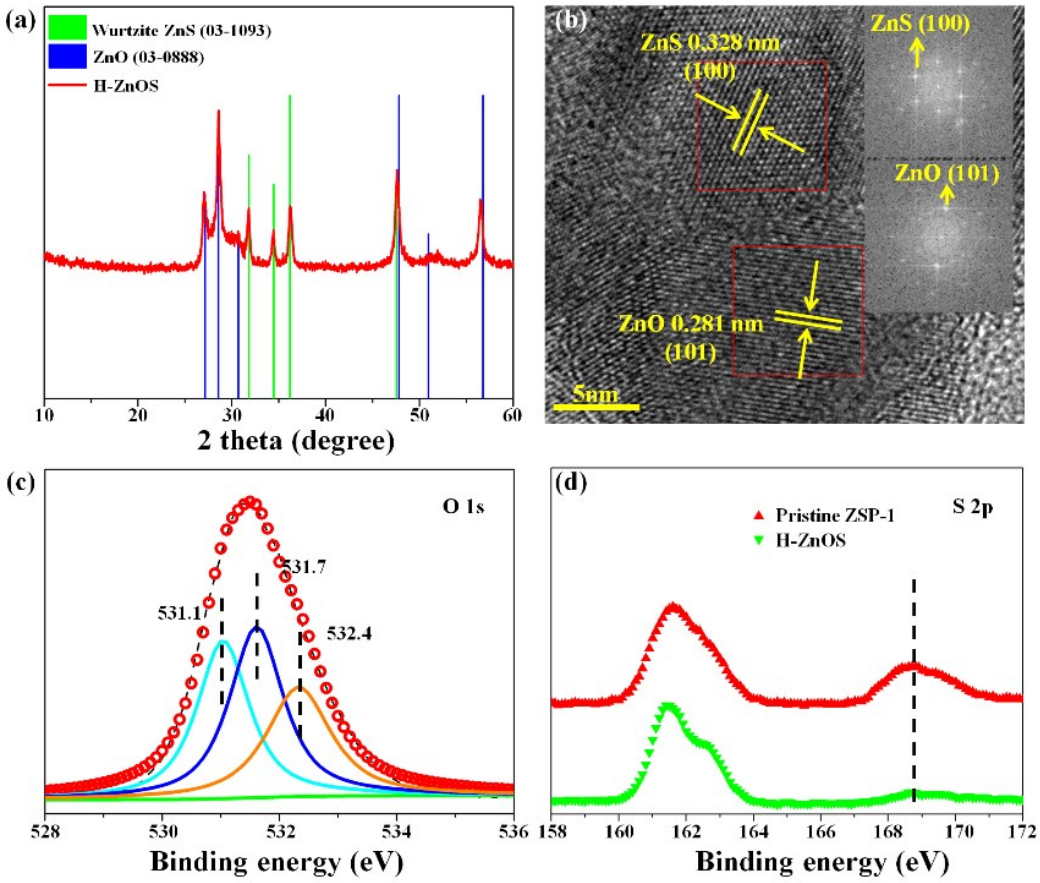

Fig. 15 (a) PXRD pattern of **H-ZnOS** and JCPDS of wurtzite ZnS and ZnO. (b) HRTEM images of **H-ZnOS**. The clear lattice spacing of 0.248 and 0.328 nm in HRTEM image are indexed to (101) plane of ZnO and (100) plane of ZnS, respectively; the inset are images of the corresponding selected area electron diffraction. (c) HRXPS spectra corresponding to O1s of **H-ZnOS**. The O 1s peak can be divided into three sub-peaks, which are consistent with that in **ZSP-1**. (d) HRXPS spectra corresponding to S 2p of **H-ZnOS**. Sharpe decrease of peak at 168.7 eV should be attributed to the decomposition of SO_4^{2-} into SO_3 and $[O^{2-}]$ species.

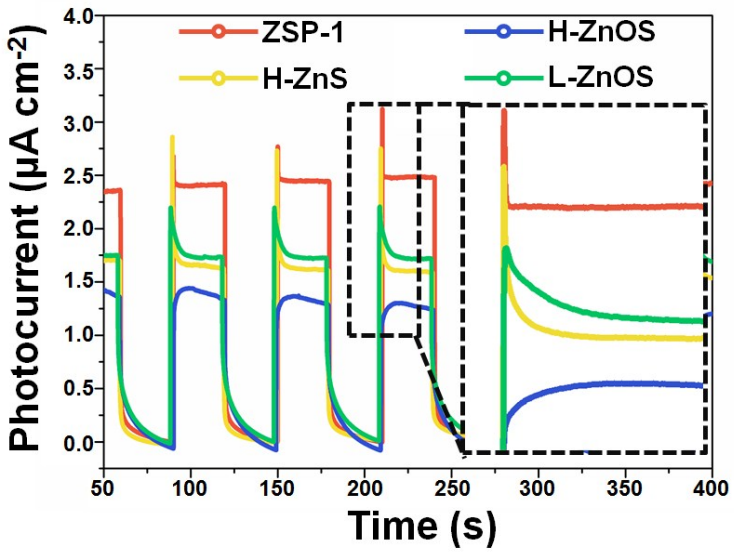

Fig. 16 (a) Photoelectric response versus time (J–t) curves for four semiconductor photoanodes, and the inset shows the enlarged transient photoelectronic response. **L-ZnOS** and pristine **ZSP-1** exhibit better photoelectric response than **H-ZnS** and **H-ZnOS**. To be noticed, **L-ZnOS** shows the slowest transient photocurrent decay rate among the four samples, which represents the instantaneous combination behavior of photogenerated electrons and holes.

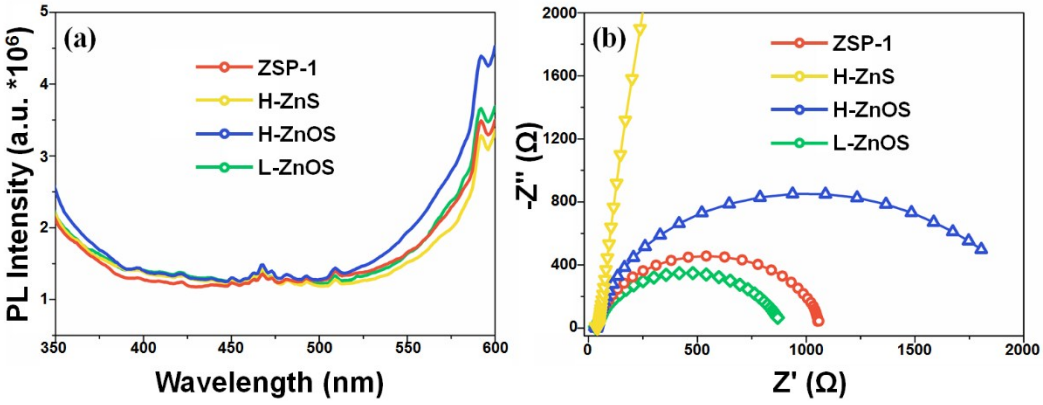

Fig. S17 (a) Photoluminescence (PL) spectra (under excitation wavelength of 310 nm) and (b) electrochemical impedance spectroscopy of different samples. No obvious PL signals were observed, indicative of effective electron-hole separation among these samples.

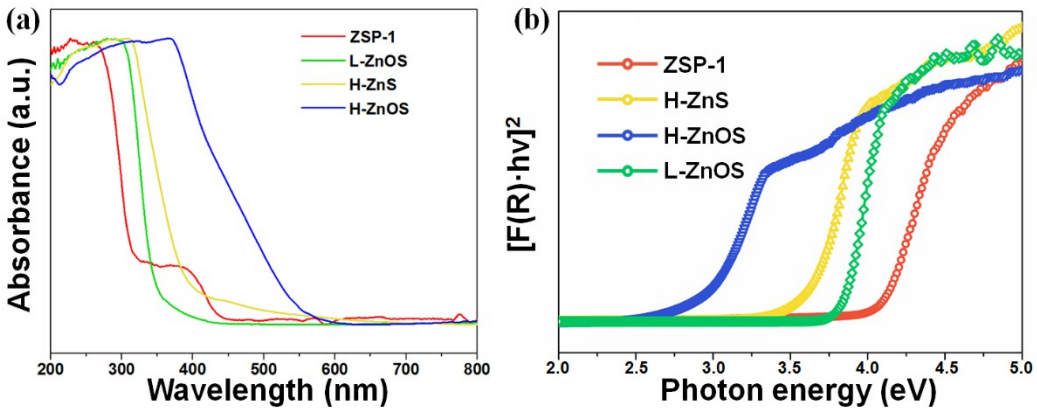

Fig. S18 (a) UV–vis absorption spectra of **ZSP-1**, **L-ZnOS**, **H-ZnS** and **H-ZnOS**. (b) Tauc plot of four as-synthesized samples derived from UV-vis DRS. Pristine **ZSP-1**, **L-ZnOS**, **H-ZnS** and **H-ZnOS** have band gap of 4.1, 3.8, 3.6 and 2.9 eV, respectively.

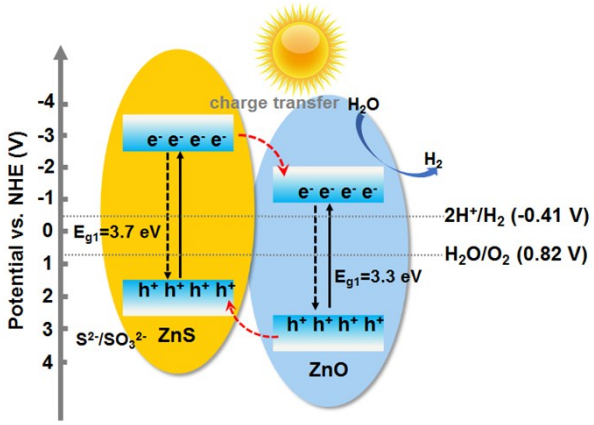

Fig. S19 Diagram illustrating the charge-transfer process in L-ZnOS during photocatalysis. The conduction band (CB) of ZnS lies on a more negative potential than that of ZnO, whereas the valence band (VB) of ZnO is more positive than that of ZnS (*CrystEngComm*, **2015**, 17, 6328–6337; *Chem. Eur. J.* **2015**, 21, 12728-12734). Under light irradiation, the photogenerated electrons from the CB of ZnS transfer into ZnO, and holes in the VB of ZnO transfer to ZnS. The electrons will be captured by H^+ on the surface of ZnO domain, which results in the formation of H_2. The existence of sacrifice reagent (Na_2S/Na_2SO_3) accelerated the consumption of photogenerated holes so that promoting the enrichment of electrons in the conduction band of ZnO.

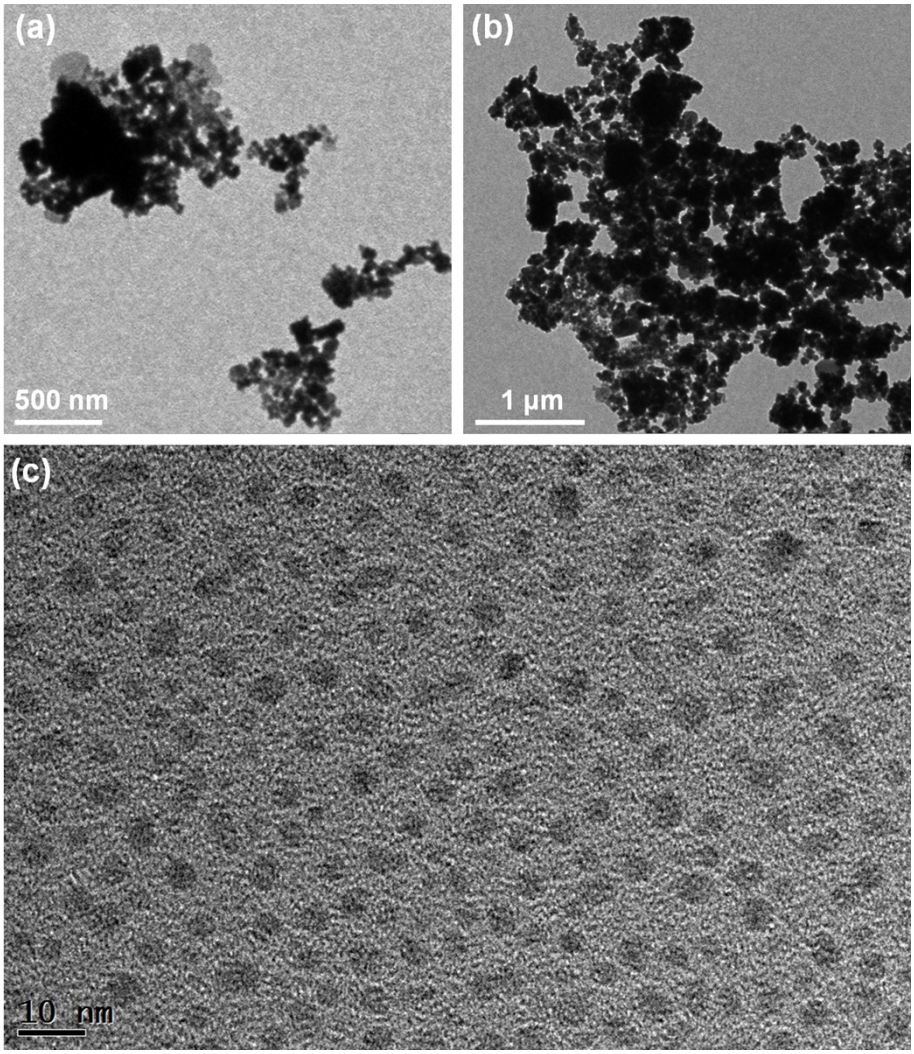

Fig. S20 Large-scaled TEM images for the dispersed **H-ZnS** (a), **H-ZnOS** (b) and **L-ZnOS** (c).

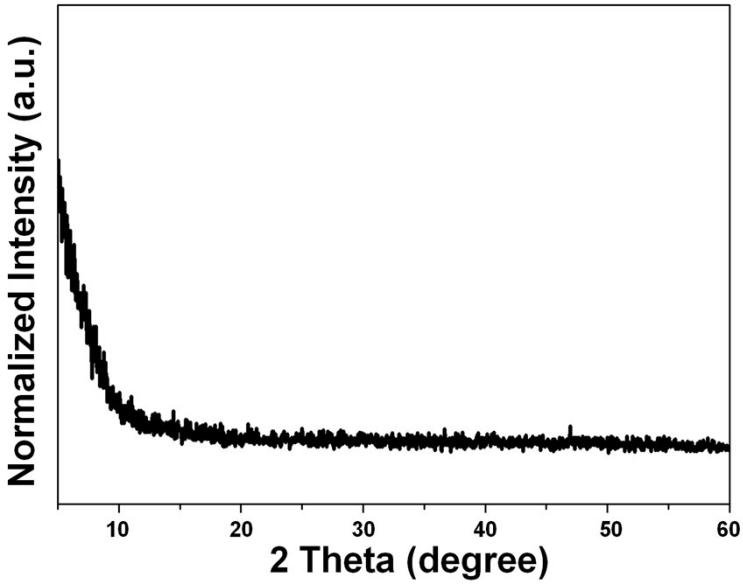

Fig. S21 PXRD pattern of **ZSP-1** after the first cycle of photocatalytic HER process.

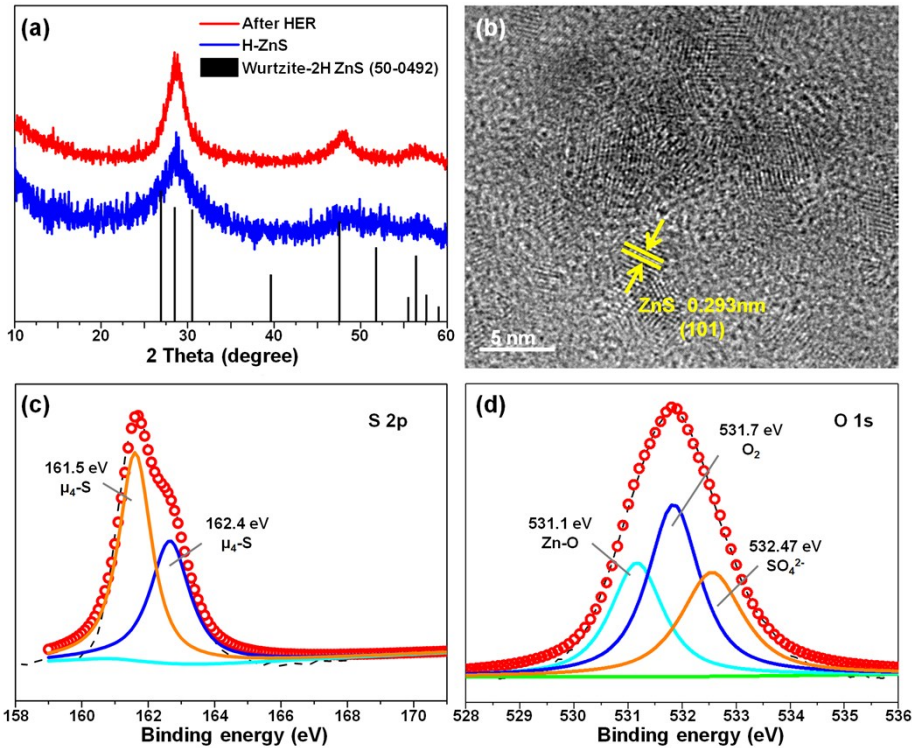

Fig. S22 (a) PXRD pattern, (b) HRTEM image, HRXPS spectra corresponding to (c) S 2p and (d) O 1s of **ZSP-1** after four cycles of photocatalytic test.

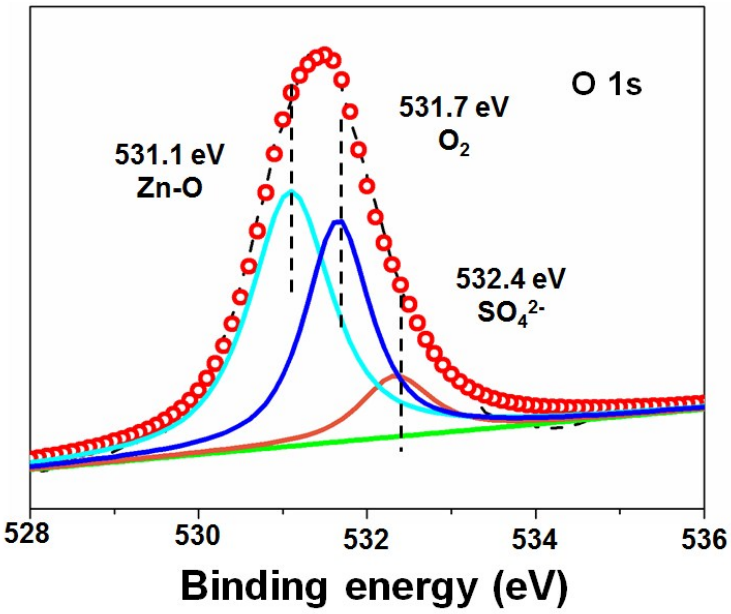

Fig. S23 HRXPS spectra corresponding to O 1s for **ZSP-1** after 20 h photocatalytic test. The enhanced peak at binding energy of 531.1 eV suggests that the existence of plenty of ZnO, which may be caused by deep oxidation of surficial ZnS phase.

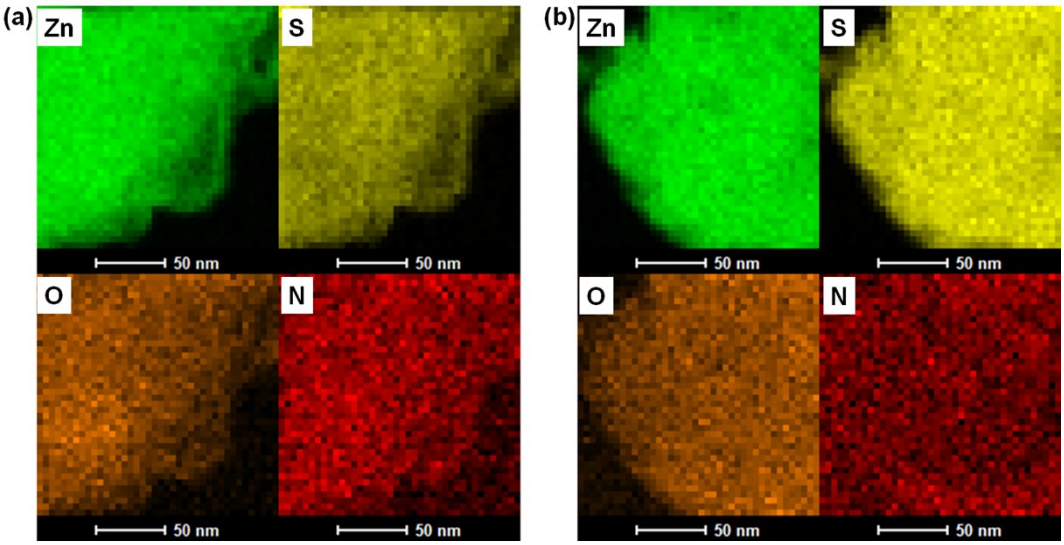

Fig. S24 EDS mapping images for **ZSP-1** after 24 h light treatment (a) and after 20 h photocatalytic test (b).

Table S1 Crystal data and structure refinement for **ZSP-1**.

Componds	**ZSP-1**
Formula	$C_{90}H_{90}N_{18}O_{24}S_{25}Zn_{25}$ (solvent)
Fw	4693.94
Crystal system	Tetragonal
Space group	*R*-3
a (Å)	28.694 (3)
b (Å)	28.694 (3)
c (Å)	36.141 (5)
α (deg)	90
β (deg)	90
γ (deg)	120
V (Å^3)	25769 (7)
Z	6
D_{calcd} (g cm^{-3})	1.815
R_{int}	0.0499
μ (mm^{-1})	3.772
F (000)	14088.0
R_1 [$I > 2\sigma(I)$]^a	0.0351
wR_2 [$I > 2\sigma(I)$]^b	0.0833
R_1 (all data)	0.0430
wR_2 (all date)	0.0884
GOF on F^2	1.057

$^aR_1 = \sum||F_o| - |F_c||/|F_o|$. $^bwR_2 = [\sum w (F_o^2 - F_c^2)^2/\sum w(F_o^2)^2]^{1/2}$.

Table S2 ZnS-based photocatalysts for photocatalytic H_2 generation.

Materials	**Morphology**	**Synthesis method**	**Sacrificial agent**	**R(H_2) (μmol g^{-1} h^{-1})**
ZSP-1	Flabellum-like cluster	Solvothermal synthesis	Na_2S/Na_2SO_3	40.0
L-ZnOS	Sub-nanoscale sphere	Light treat ZSP-1	Na_2S/Na_2SO_3	94.0
H-ZnS	Nanoparticle	Thermal treat ZSP-1	Na_2S/Na_2SO_3	1.7
H-ZnOS	nanoparticle	Thermal treat ZSP-1(O_2)	Na_2S/Na_2SO_3	21.4
ZnO/ZnS [1]	Nanorod	Anion exchange reaction	Glycerol	19.2
ZnO/ZnS [2]	Nanowire	Solvothermal synthesis	Na_2S/Na_2SO_3	59.3
ZnO/ZnS [3]	Nanoparticle	Sulfuration of MOF-5	Na_2S/Na_2SO_3	11.6-415.3
ZnS [4]	Nanoparticle	Solvothermal reaction	Lactic acid	17.5

Reference:

1. D. Bao, P. Gao, X. Zhu, S. Sun, Y. Wang, X. Li, Y. Chen, H. Zhou, Y. Wang, P. Yang, *Chem. Eur. J.* 2015, **21**, 12728-12734.

2. X. Gao, J. Wang, J. Yu, H. Xu, *CrystEngComm*, 2015, **17**, 6328-6337.

3. X. Zhao, J. Feng, J. Liu, J. Lu, W. Shi, G. Yang, G. Wang, P. Feng, P. Cheng, *Adv. Sci.* 2018, **5**, 1700590.

4. Z. Fang, S. Weng, X. Ye, W. Feng, Z. Zheng, M. Lu, S. Lin, X. Fu, P. Liu, *ACS Appl. Mater. Interfaces* 2015, **7**, 13915-13924.